RI 9418

REPORT OF INVESTIGATIONS/1992

Canopy and Base Load Distribution on a Longwall Shield

By Thomas M. Barczak and David F. Gearhart

UNITED STATES DEPARTMENT OF THE INTERIOR

BUREAU OF MINES

Report of Investigations 9418

Canopy and Base Load Distribution on a Longwall Shield

By Thomas M. Barczak and David F. Gearhart

UNITED STATES DEPARTMENT OF THE INTERIOR
Manuel Lujan, Jr., Secretary

BUREAU OF MINES
T S Ary, Director

Library of Congress Cataloging in Publication Data:

Barczak, Thomas M.

Canopy and base load distribution on a longwall shield / by Thomas M. Barczak and David F. Gearhart.

p. cm. — (Report of investigations; 9418)

Includes bibliographical references.

Supt. of Docs. no.: I 28.23:9418.

1. Mine roof control. 2. Dead loads (Mechanics). 3. Longwall mining. I. Gearhart, David F. II. Title. III. Series: Report of investigations (United States. Bureau of Mines); 9418.

TN23.U43 [TN288] 622 s—dc20 [622'.28] 92-5711 CIP

CONTENTS

ILLUSTRATIONS

UNIT OF MEASURE ABBREVIATIONS USED IN THIS REPORT

ft	foot	lb	pound
ft^2	square foot	pct	percent
in	inch	psi	pound per square inch
in^2	square inch	ton/ft^2	ton per square foot

CANOPY AND BASE LOAD DISTRIBUTION ON A LONGWALL SHIELD

By Thomas M. Barczak[1] and David F. Gearhart[2]

ABSTRACT

This U.S. Bureau of Mines report examines the roof and floor contact pressure provided by the interaction of a shield with the surrounding strata. Controlled forces were applied to an 800-ton two-leg shield in the Bureau's mine roof simulator; the distribution of forces acting on the canopy and base of the shield were measured with 24 hydraulic pressure cells. Several influential factors that affect the load distribution were investigated: (1) the magnitude of loading (leg pressure); (2) the profile of the canopy, principally the upward-sloping tip; (3) the base-lifting device; (4) horizontal load acting on the shield; and (5) compliancy of the immediate roof and floor. It was concluded that the shield does not develop full canopy or base contact without deformation of the strata. Maximum contact pressures are developed at the rear of the canopy and on the toes of the base. Less than 10 pct of the available shield capacity is developed at the canopy tip despite the design intention to ensure tip contact. Horizontal loading reduced the toe pressure acting on the base by as much as 75 pct. The base-lifting device exaggerated the inherently high toe loading, increasing the contact pressure by more than 200 pct.

[1]Research physcist, Pittsburgh Research Center, U.S. Bureau of Mines, Pittsburgh, PA.
[2]Electrical engineer, Schneider Services International, Pittsburgh, PA.

INTRODUCTION

This work was done in support of the U.S. Bureau of Mines' goal to improve the health and safety of underground coal mining through development of better roof support systems.

Successful application of the longwall mining method requires the use of high-capacity face support structures to provide adequate ground control. State-of-the-art shield supports provide capacities of up to 900 tons of (vertical) supporting force. The use of these high capacities requires correspondingly large canopy and base contact areas to distribute the force to the mine roof and floor. Although the resulting average force per area (contact pressure) is relatively low (10 to 12 ton/ft^2 or about 140 to 170 psi for the canopy and 30 to 40 ton/ft^2 or about 400 to 600 psi for the base), the actual contact interaction causes unevenly distributed and much higher contact pressures. When the maximum of these distributions exceeds certain values, local failures of the roof and floor might follow. Such failures could degrade strata stability and make support advancement difficult. To prevent this occurrence, a better understanding of load distribution between longwall shields and the contacting strata is required.

Assessment of a shield's roof and floor contact pressure can be made by some form of mathematical model or by experimental means. The most commonly used mathematical model assumes a rigid structure yielding a linear pressure profile along the length of the canopy or base as shown in figure 1.[3] However, this provides an erroneous picture of the load distribution since the structures are known to deform from loading. Unfortunately, numerical models that have been developed to model the elastic response of the shield components have met with only limited success. Hence, an experimental approach was chosen for this study. The approach used was to employ a series of hydraulic pressure cells distributed on the canopy and base to measure the contact pressure under known loading conditions provided by the Bureau's 3-million-lb load frame.

The objective of this study was to evaluate the load distribution acting on a shield for simulated underground conditions. This requires some consideration of the compliancy of the roof and floor, since the deformation of the strata can influence the contact area on the shield and the corresponding canopy and base load distribution. The rigid steel platens of the load frame can simulate very stiff strata, such as might be encountered with a strong sandstone or limestone structure, but the platens do not simulate more compliant strata, such as shale or clay formations. The compliancy of the immediate roof and floor were simulated by wood or rubber layers placed between the shield and the platens of the load frame. Wood and rubber were chosen primarily for practical reasons, but they do have properties similar to (broken) rock in that they increase in stiffness as they are compressed. Other parameters that were investigated in the study included (1) contact configurations established by the placement of the load cells on the canopy and base; (2) amount of external horizontal force acting on the shield; (3) applied vertical force; and (4) canopy capsule force. The effects of a base-lifting device were also investigated as part of this study.

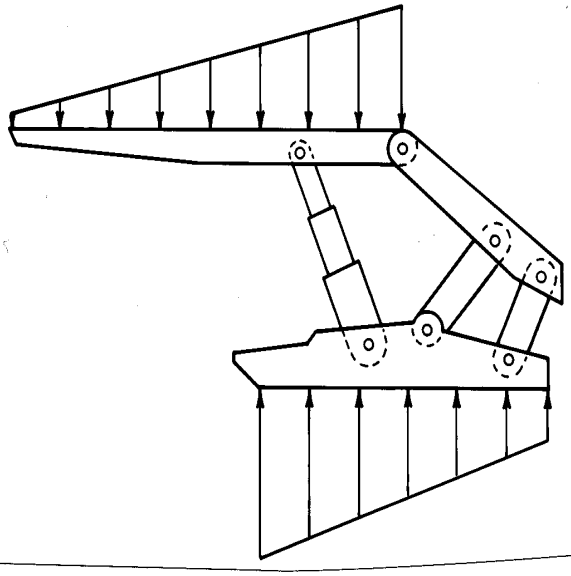

Figure 1.—Linear force distribution assuming rigid body structure.

[3]Peng, S. S. Coal Mine Ground Control. Wiley, 1978, pp. 259-268.

ACKNOWLEDGMENTS

The authors wish to acknowledge Island Creek Coal Co., in particular Rau Pothini, longwall coordinator, for supplying the shield used in this study. This work was a cooperative effort established between the Bureau, West Virginia University, and Island Creek Coal Co. Gratitude is also extended to Syd Peng, chairman, Department of Mining Engineering, West Virginia University, for his assistance in organizing this effort.

ASSESSMENT OF INFLUENTIAL FACTORS

An investigation of a longwall shield's canopy and base load distribution under controlled laboratory conditions requires a fundamental understanding of influential factors. These factors are divided into three general categories: (1) boundary conditions, which describe the interaction of the shield with the strata; (2) shield design, which describes the component constructions and overall shield mechanics; and (3) load-measurement devices that are used to measure the contact pressure.

BOUNDARY CONDITIONS

The interaction of a shield with the immediate roof and floor imposes boundary conditions that control shield loading. These boundary conditions are established by (1) the contact configuration established with the immediate roof and floor; (2) loading induced by the strata; and (3) the deformation of the roof and floor in response to the shield resistance.

The contact configuration established with the immediate roof and floor can range from full contact over the entire canopy and base surface area to isolated point contact at a few locations. From analysis of force and moment equilibrium of the shield, it is readily seen that the contact configuration largely determines the magnitude and distribution of forces imposed on the shield by the strata interaction.

After being actively set against the roof, the shield becomes a passive support, and load is developed in response to support and strata interactions that produce displacements of the shield canopy relative to the base.[4] As illustrated in figure 2, both vertical and horizontal forces can be imposed on the shield by roof-to-floor and face-to-waste displacements of the strata or by resistance of the strata to internal shield forces that produce motion of the canopy relative to the base. A shield acted upon by vertical forces has a different loading distribution on the canopy and base than a shield acted upon by both vertical and horizontal forces does. Therefore, it is necessary to control both vertical and horizontal shield loading in the laboratory and to understand the source of this loading to fully evaluate the distribution of forces transmitted to the roof and floor.

Shield canopy and base components are not rigid structures and the immediate roof and floor are generally not rigid foundations. Therefore, a rather complex boundary condition is developed involving the interaction of the support with the strata. The distribution of forces acting on the shield is determined by the elastic deformation of the shield components and the compliancy of the immediate strata in response to the shield resistance. Likewise, the contour of the immediate roof and floor may not coincide with the profile of the canopy and base, causing isolated areas of contact. The capacity of the strata to deform to establish more uniform contact with the canopy and base significantly influences the resulting loading distribution in these situations. Hence, a stiff competent roof with a well-defined contact boundary produces a much different loading distribution on the shield canopy than a friable roof with a compressible layer of debris over much of the canopy does. Likewise, a strong floor is more likely than a weak floor to produce localized areas of high stress concentration on the base. Soft floor materials, such as clay, exhibit plastic deformation in response to base loading and conform more easily to the profile and elastic response of the base structure.

SHIELD DESIGN

The design of a shield is also an important consideration in assessing shield loading and strata interaction. The primary considerations are (1) the location of the leg connection relative to the length of the canopy and base; (2) the arrangement and loading of the lemniscate links; (3) the profile and bending stiffness of the canopy and base.

[4]Barczak, T. M., and D. E. Schwemmer. Horizontal and Vertical Load Transferring Mechanisms in Longwall Roof Supports. BuMines RI 9188, 1988, 24 pp.

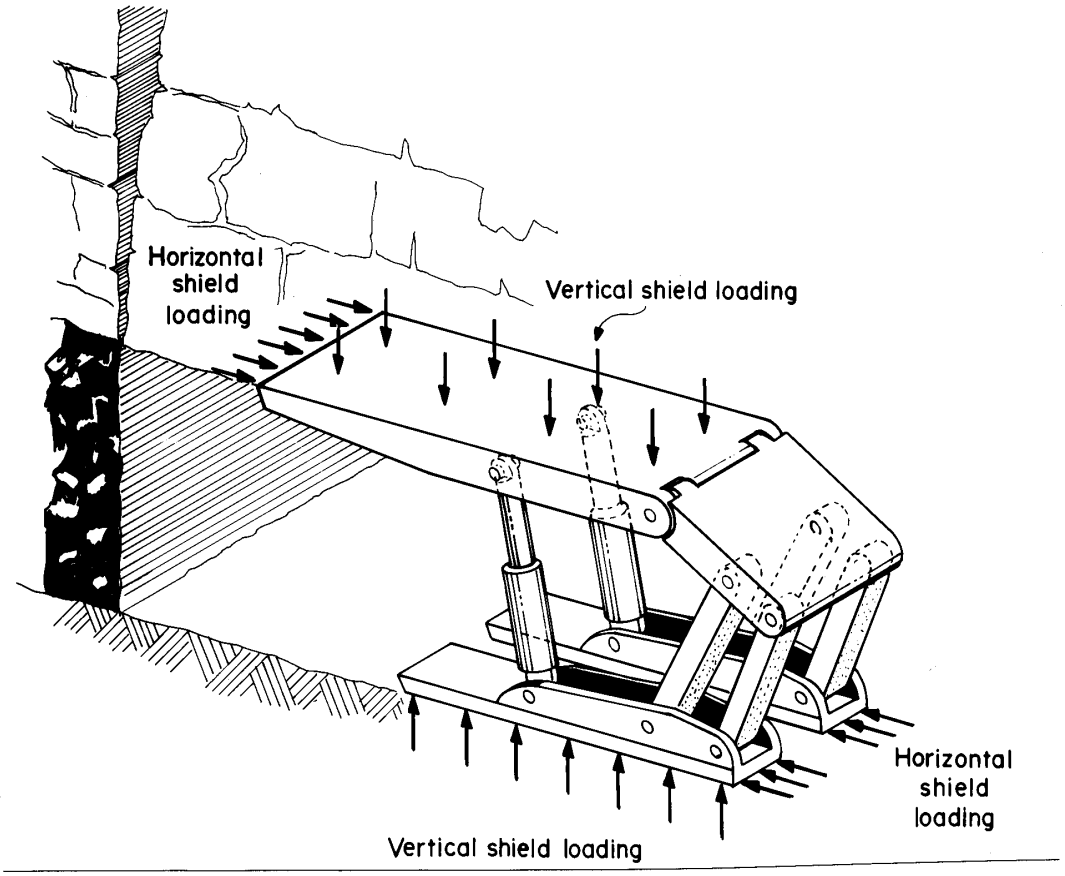

Figure 2.—Horizontal and vertical forces acting on shield support.

A study of shield mechanics indicates that the leg is the dominant internal force acting on the shield canopy.[5] This suggests that the location of the resultant external force acting on the canopy is likely to be in close proximity to the leg connection, since the canopy capsule force and the reaction developed at the caving shield joint are of much smaller magnitude than the leg forces. The distribution of loading on the canopy is largely determined by the relative length of canopy forward and rearward of the leg connection. Typically, considerably less loading is developed at the tip of the canopy than at the rear, since the tip portion is considerably farther from the leg and requires proportionally less force to maintain moment equilibrium.

The distribution of forces is also dependent upon the bending stiffness of the canopy. A perfectly rigid canopy and base provide a linear distribution of loading as illustrated in figure 1, while an elastic structure might respond as shown in figure 3 in accordance with deformations produced by internal and external forces. To ensure contact pressure at the canopy tip, there has been a recent trend in shield design to slope the tip portion of the canopy upward with respect to the remainder of the canopy as shown in figure 4. For example, the shield utilized in this study had a tip distortion of approximately 2 in. Initially, this produces two-point contact at the tip and rear of the canopy. Generally, for this type of design, elastic deformation of the canopy does not produce full contact along the length of the canopy. Hence for this type of canopy design, deformation of the strata is necessary to establish full canopy contact.

Since the canopy is cantilevered in front of the toe of the base and the leg connection on the canopy is forward of the leg connection on the base, there is a natural tendency for a rotational moment (see figure 5) that produces high toe loading in two-leg shield designs. The link forces

[5]Barczak, T. M., and D. E. Schwemmer. Two-Leg Longwall Shield Mechanics. BuMines RI 9220, 1989, 34 pp.

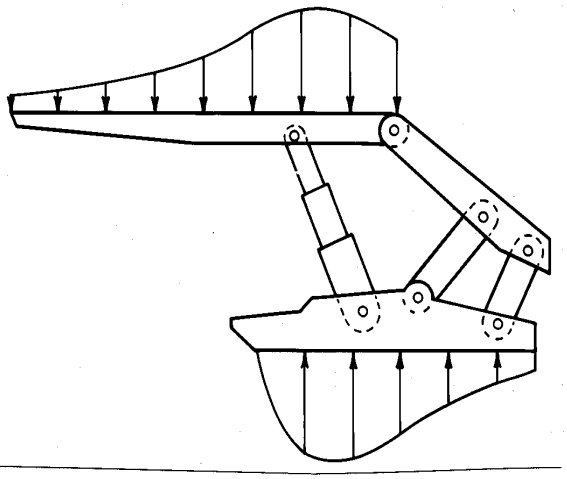

Figure 3.—Possible load distribution assuming elastic support structure.

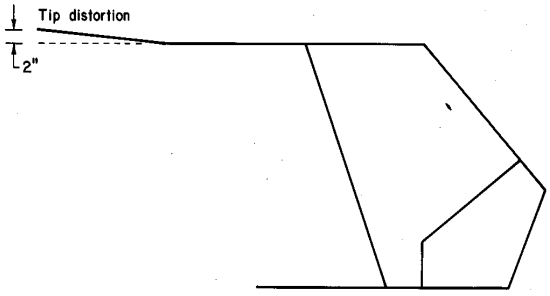

Figure 4.—Upward sloping of canopy tip to ensure tip contact.

acting in conjunction with the leg forces provide moment equilibrium of the base. Since the rear link acts in opposite direction to the leg, a resultant force forward of the leg is possible. The location of the resultant force is largely dependent upon the relative magnitude of the leg and link forces.[6]

Because of the relatively high load distribution at the toe of the shield, which often causes the base to sink into the floor, another trend in shield design has been the incorporation of a base-lifting device as shown in figure 6. The base-lifting plates are extended by single acting hydraulic cylinders that lift the toes of the base during the support advance. After the support is advanced, the plates are retracted to rest against the bottom of the base, creating a discontinuity near the toe of the base. This arrangement promotes two-point contact at the toe and rear of the base similar to that produced on the canopy by the

[6]Barczak, T. M., and R. C. Garson. Shield Mechanics and Resultant Load Vector Studies. BuMines RI 9027, 1986, 43 pp.

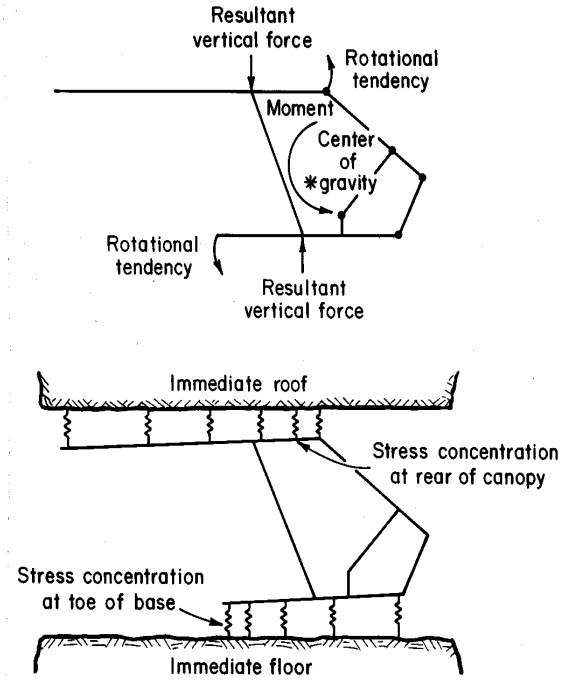

Figure 5.—Rotational moment (top) causing high toe loading (bottom) in two-leg shield design.

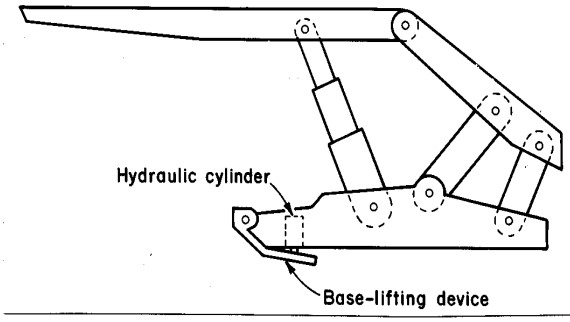

Figure 6.—Base-lifting device.

sloping of the canopy tip. However, bases tend to have higher bending stiffness than canopy structures and are less likely to deform from loading. Therefore, deformation of the floor is even more critical to establish full contact along the length of the base. In hard floor conditions, the presence of the base-lifting device can exaggerate the inherently high stress concentration at the toe of the base. Fortunately, quite often there is debris or soft floor material that compacts to conform to the base geometry to alleviate the two-point contact loading.

LOAD-MEASUREMENT DEVICES

Since load-measurement devices interface with the immediate strata and the shield, they become an integral part of the system and influence the resulting load distribution. The load-measurement devices must be employed in such a way that the entire load is transferred through these devices to preserve force equilibrium. Under this condition, the placement of the load cells alone defines the contact configuration and contact area, which, as previously discussed, is a major factor influencing the magnitude and distribution of the forces acting on the shield.

The load cells should also be calibrated to preserve the accuracy of the load measurements. Some information should also be obtained pertaining to the stiffness of the load-measurement devices. In areas where there is no rotational degree of freedom within the shield component, the relative stiffness of the load cells may influence the resulting loading distribution. For example, when multiple cells are closely placed between the leg and the rear of the canopy, a cell(s) surrounded by stiffer cells tends to attract less force. While force equilibrium is preserved, the distribution of this force may be affected by this behavior. This situation is most likely to occur when a rigid boundary roof condition exists. Therefore, if several load-measuring cells are employed, the relative stiffness of the load cells should be similar. A more critical consideration in rigid boundary roof conditions is that slight irregularities in the surface of the canopy and base can produce localized areas of high stress concentrations, particularly when very stiff load cells are employed.

LABORATORY SIMULATIONS

Laboratory simulations were conducted in the Bureau's mine roof simulator. The simulator, shown in figure 7, is capable of providing controlled forces or displacements in both a vertical and horizontal direction to full-sized longwall shields. The biaxial load frame has a force capacity of 3 million lb vertically and 1.6 million lb horizontally. A total of 45 tests were conducted.

A two-leg 800-ton shield provided by Island Creek Coal Co. was used for this study. This shield is a high-capacity support representative of state-of-the-art two-leg shield designs. It has a canopy contact area of 59.2 ft^2 and a total base contact area of 24.6 ft^2 from two base pontoons.

TEST INSTRUMENTATION AND CALIBRATION

Hydraulic pressure cells were used to measure the load distribution acting on the shield canopy and base. The cells are constructed of two parallel 6-in by 6-in stainless steel plates. The plates are welded along the circumference and filled with oil to provide a flatjack arrangement as shown in figure 8. The cells are fitted with a tube that is connected to a pressure transducer for measurement of the hydraulic pressure developed in the cell. Since the cell is a closed system, deformation of the cell produced by loading on the plate surfaces produces an increase in hydraulic pressure.

Twenty-four pressure cells of this construction were employed to measure the canopy and base load distribution on the longwall shield. Each cell was calibrated to a force of 300,000 lb. The calibrations were made in a stiff 1-million-lb load frame. The accuracy of the load cells ranged from 0.3 to 12.5 pct and averaged 2.4 pct for the 24 load cells. This equates to an error of 2.4 tons at 100 tons of measured load. An example of the stiffness of the load cells is shown in figure 9. The stiffness is seen to increase nonlinearly with increasing load, probably because of some air in the cell system.

DATA DOCUMENTATION

Test data are documented in several ways throughout the report. A brief explanation of data documentation follows.

1. Measured Load Profiles.—These graphs depict load cell response as a function of location on the shield. Different curves are shown for 1,000-psi increments of leg pressure. These graphs are useful in showing load transfer to different portions of the canopy or base from deformation of the contact material (simulated roof or floor) or deformation of the shield structure.

2. Resultant Loading.—The location of the resultant force acting on the canopy or base is shown as a function of leg pressure for each test. Analysis of these data shows movement of the resultant external force along the length of the canopy or base for different load conditions. While the location of the resultant force is not generally the point of maximum pressure and is not unique to one contact configuration, it is determined by moment equilibrium of the loading distribution and therefore provides some indication of the nature of the loading. Changes in the location of the resultant are indicative of a change in load distribution. These curves are useful in determining a shift in loading toward the front or rear of the shield.

3. Contact Pressure Profiles.—Measured force from each of the load cells is distributed over the entire area of the canopy or base as an approximation of contact pressure for full-contact load conditions. Force equilibrium is

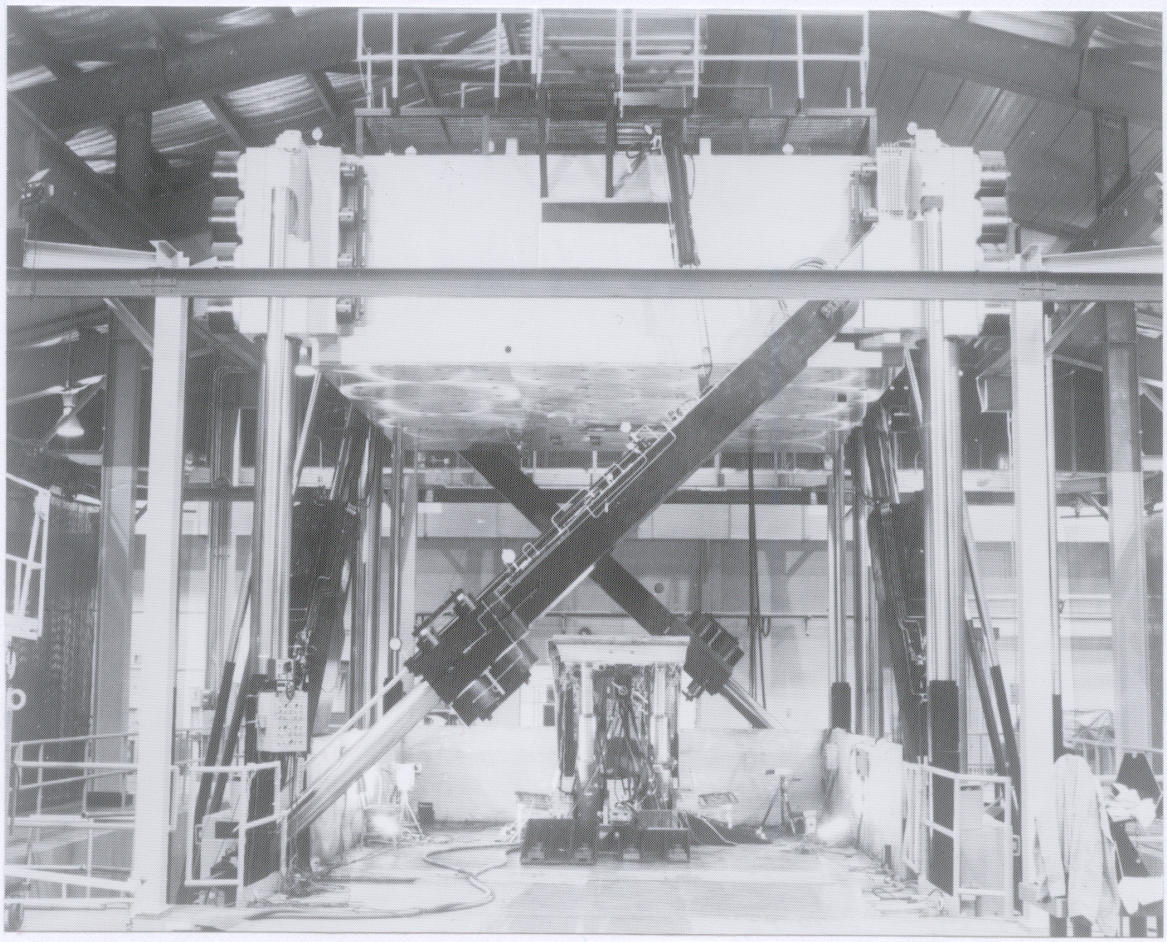

Figure 7.—Mine roof simulator.

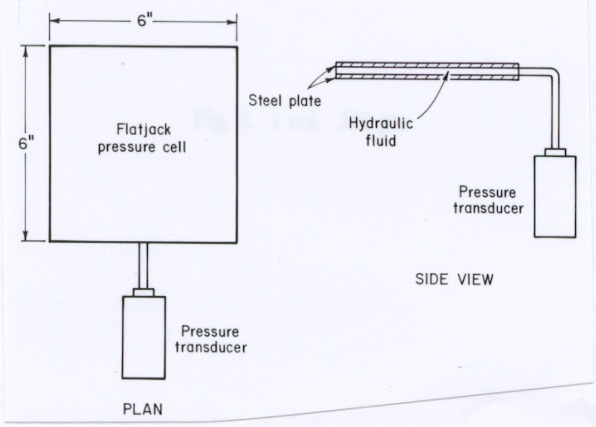

Figure 8.—Hydraulic pressure cell used to measure load distribution.

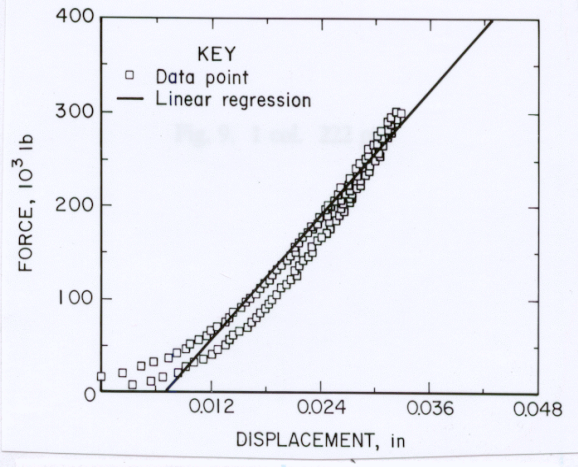

Figure 9.—Example of stiffness of pressure cell.

preserved in the distribution process by distributing the measured load cell forces in proportion to the area of the cells relative to the area of the canopy or base so that the total force remains a constant. A description of the stress contour method is provided in the appendix.

DATA ANALYSIS AND TEST RESULTS

The tests are categorized in three areas determined by the employment of the load-measurement devices: (1) canopy distribution studies, (2) base distribution studies, and (3) combined canopy and base distribution studies.

Canopy Tests

A total of 10 tests were conducted to measure the loading distribution on the canopy. Parameters investigated during this test series included (1) contact configuration, (2) stiffness of the roof boundary, and (3) horizontal shield loading. Three different canopy contact configurations, as shown in figure 10, were investigated. Full base contact was utilized for all canopy tests. Wood and rubber were utilized to simulate the compliance of the immediate roof to assess the impact of strata deformations on the canopy load distribution. Horizontal loads are developed by the platens of the load frame resisting the horizontal motion of the canopy and base caused by the action of the leg forces. By allowing the load frame platens to freely displace in the horizontal direction, the horizontal loading on the shield was eliminated for certain tests to determine the effect of the horizontal loading on the distribution of forces acting on the canopy.

The profile of the canopy causes the canopy tip and rear to contact first, which causes initial load development at the front and rear of the canopy. As shown in figure 11, the canopy does not bend sufficiently to cause contact over the full length of the canopy. In this test, the shield reacted against the rigid steel platens of the load frame to simulate a hard flat roof structure that does not deform from the shield contact pressure. Contact was established over about 40 pct of the canopy for leg pressures up to 4,500 psi. At this magnitude of loading, there is no contact directly above the leg, which is located approximately 4 ft from the rear of the canopy, and no contact 2 ft from the tip of the canopy. Hence, there exists a span of about 7.5 ft in the middle portion of the canopy that never establishes contact under these load conditions. While loading above 4,500 psi was not attempted for these specific tests, the data suggest that full canopy contact would not be attained when the shield is reacting against a flat stiff surface even at yield leg pressure.

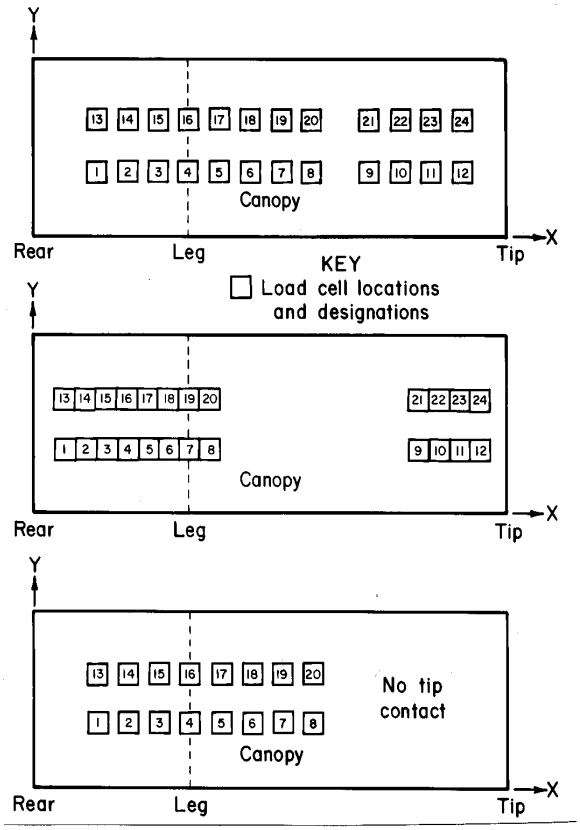

Figure 10.— Canopy contact configurations for canopy load distribution tests.

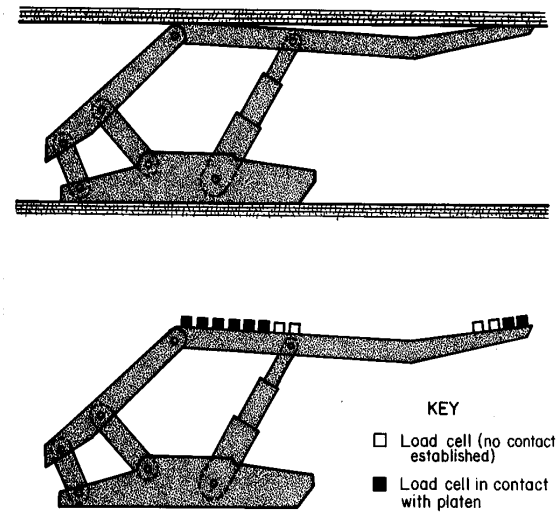

Figure 11.—Contact area established against rigid roof. Top, exaggerated view of canopy distortion; bottom, load measuring cells on canopy.

To simulate immediate roof conditions where the strata deform under load, wood or rubber layers were placed between the load cells and the platens. The contact area on the canopy increases as the wood or rubber is compressed from the forces acting on the shield. The contact area increased from 40 pct for the rigid roof simulations discussed above to about 90 pct for the wood and 100 pct for the rubber contact materials. The location of the contact force migrates from the ends (tip and rear) of the canopy toward the leg as the canopy and simulated roof material deform. In rigid roof simulations, the maximum contact force at the rear of the canopy also moves inward toward the leg as the loading increases. A comparison of load development on the canopy for rigid and compliant roof simulations is shown in figure 12. Maximum contact pressures developed on the canopy are significantly higher for stiffer roof structures, since more of the loading is concentrated on a smaller area of the canopy (see figure 13).

The load distribution on the canopy is measured by the 24 load cells arranged in 2 lines of 12 cells along the length of the canopy (see figure 10). Since the 24 load cells define a contact area of about 10 pct of the total area of the canopy, roof contact pressures as determined from the load cell data are magnified by a factor of 10 (assuming all load cells are in contact throughout the loading) in comparison to full canopy contact over its entire surface. Therefore, to provide a more realistic expression of roof contact pressures, the load cell forces were distributed over the entire surface of the canopy using a stress contour software program. A description of the stress redistribution technique is provided in the appendix. Several observations are made regarding these pressure profiles:

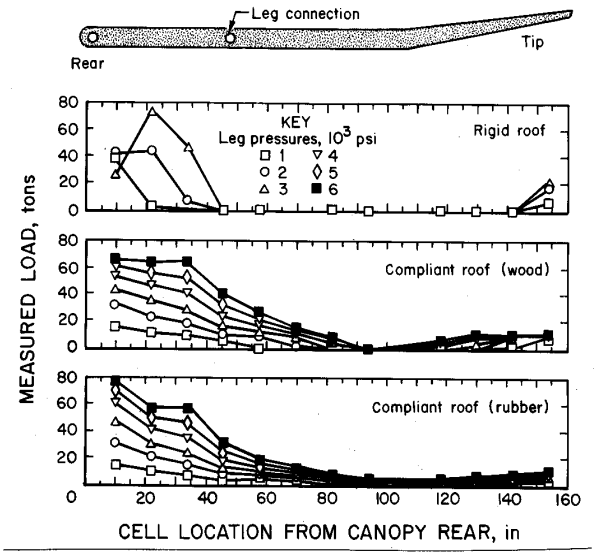

Figure 12.—Comparison of canopy loading for rigid and compliant roof simulations.

1. In general, the pressure increases nonlinearly from the tip of the canopy to the rear as shown in figure 14. A

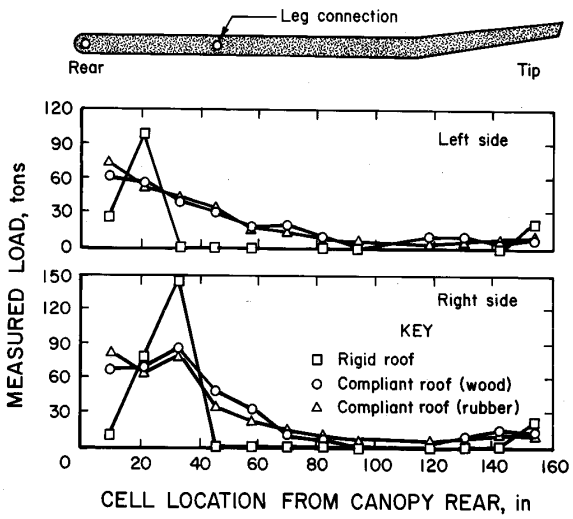

Figure 13.—Maximum canopy contact loading for stiff and compliant roof simulations.

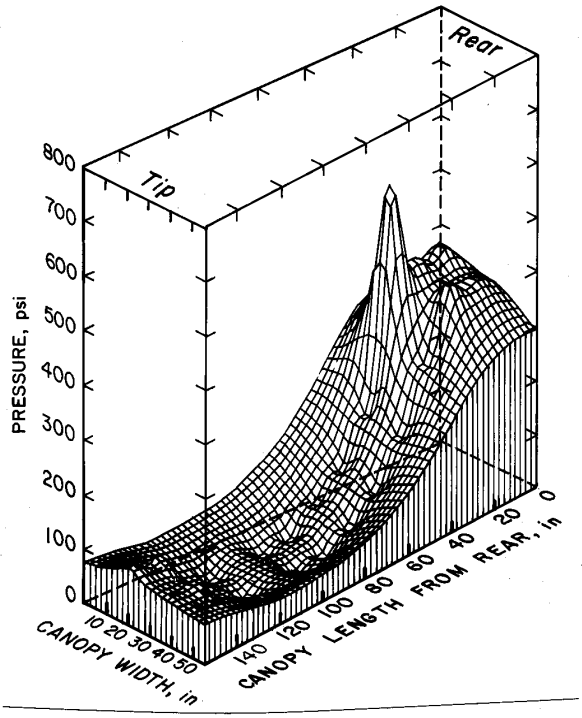

Figure 14.—Contact pressure profile for canopy.

more detailed examination shows that the minimum pressure develops in the region where the canopy begins to slope upward, creating an inflection point of minimum pressure in the pressure profile. From this inflection point the pressure rises slightly to the tip and increases at a much faster rate while progressing to the rear of the canopy.

2. There is relatively little contact pressure developed at the canopy tip compared with the rear area of the canopy, regardless of the contact configuration. Two things are responsible for this behavior: (1) Since the tip of the canopy is 2.25 times as far from the leg as the rear edge of the canopy, only 44 pct of the force at the rear of the canopy is required at the tip of the canopy to maintain equilibrium (assuming a rigid canopy with point loading at the front and rear ends); and (2) Because of the geometry of the canopy with the tip inclined upward, more contact is developed at the rear of the canopy than near the tip of the canopy as loading increases, which further reduces the forces required forward of the leg to maintain moment equilibrium.

3. When full contact is established along the length of the canopy, contact pressures of about 50 to 75 psi can be expected at the tip of the canopy at leg pressures above 6,000 psi and pressures of about 300 to 350 psi at the rear. For stiff immediate roof boundaries where full contact is not established over the entire canopy, localized areas of pressure approaching 1,000 psi may develop, typically near the rear of the canopy.

4. Tests were also conducted in which the sloped portion of the canopy was not in contact with the load frame. This contact configuration may be caused by a layer of debris on the flat portion of the canopy or by the presence of cavities in the immediate roof that prevent tip contact. The pressure profile for this configuration is similar to the full-contact configuration where tip loading was present, except the load is more uniformly distributed with higher loads in front of the leg than occurred in the full-contact configuration.

A free-body diagram of the canopy as shown in figure 15 indicates that there are three internal forces acting on the canopy: (1) leg force, (2) canopy capsule force, and (3) canopy-caving shield joint force. Since the caving shield assembly has very little vertical stiffness and the area of the canopy capsule is small, these components develop little force and the leg becomes the dominant force acting on the canopy. Therefore, the resultant external force induced by the roof contact must be near the leg connection to maintain moment equilibrium.

The resultant consistently migrates toward the leg as loading increases from zero leg pressure, and generally is positioned slightly rearward of the leg as shown in figure 16 as the pressure approaches yield pressure. The tests indicate that the resultant begins significantly rearward of the leg and migrates forward toward the leg for stiff flat roof conditions, while for softer roof conditions, as simulated by the wood or rubber interface material, the resultant begins forward of the leg and migrates rearward to a point slightly past the leg. This difference in the direction of resultant load migration is explained by examination of the load distribution. As shown in figure 17, load development at the rear of the canopy in the stiff roof simulation is confined initially to small contact areas that progress toward the leg as leg pressures increase. This

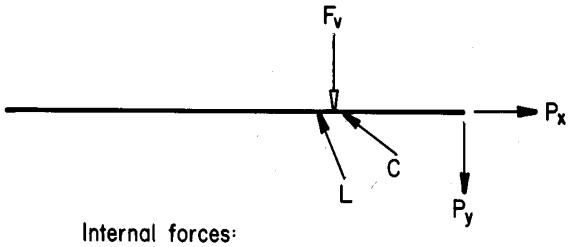

Internal forces:
L = leg force
C = canopy capsule force
P_x, P_y = caving shield joint reaction

External forces:
F_V = resultant canopy force

Figure 15.—Free-body diagram of shield canopy.

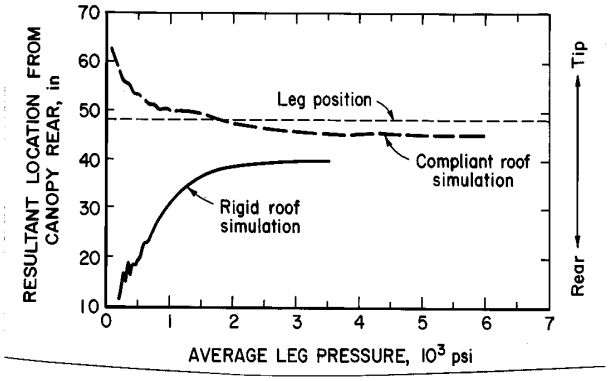

Figure 16.—Movement of canopy resultant as shield loading increases.

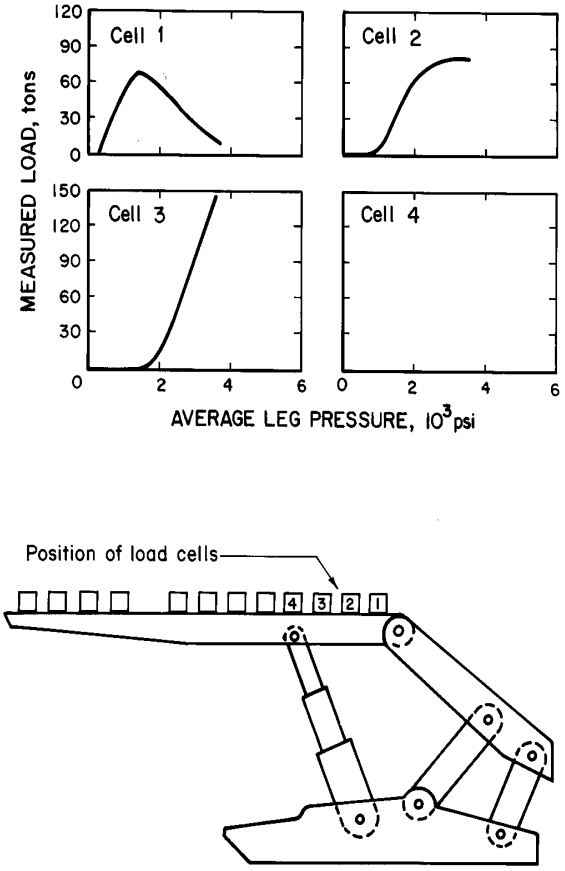

Figure 17.—Migration of load development at rear of canopy for rigid roof simulation.

explains the movement of the resultant forward. In contrast, load development during the weak roof simulation occurred over a larger area, but the load development at the rear of the canopy increased at a faster rate than at the tip of the canopy. This explains the movement of the resultant toward the rear for weak (compliant) roof conditions.

When the canopy was permitted to displace toward the face without external resistance to eliminate horizontal shield loading, slightly less contact load was observed in front of the leg, and slightly higher loads were observed to the rear of the leg. This caused the resultant location to move toward the rear of the canopy. When the external horizontal force is removed, the resultant tends to shift toward the rear of the support to offset the moment created from the line of action of the vertical forces acting on the canopy and base (see figure 4). A comparison of resultant locations and calculated pressure profiles with and without horizontal loading is shown in figure 18.

Base Tests

A total of 22 tests were conducted to evaluate the contact pressure on the base of the shield. The effect of three parameters on the resulting load distribution were evaluated: (1) horizontal loading, (2) the base-lifting device, and (3) the location of the resultant canopy force. Full base contact using 24 load measuring cells (12 on each base pontoon) were utilized for all tests. All tests employed wood or rubber under the load cells to simulate floor deformation. Rigid floor conditions were not simulated.

Horizontal loading is typically generated from the internal leg forces and the restraining frictional force imposed by the immediate roof and floor. When the canopy is permitted to displace forward toward the face without external resistance, no horizontal loading is generated. Without horizontal loading, the resultant vertical force acting on the base must be coincident with the resultant vertical force acting on the canopy. Since the canopy resultant is located near the leg connection, this places the resultant vertical force acting on the base at about 75 in from the rear of the base or 21 in from the toe.

The effect of an externally applied horizontal load is to push the resultant further toward the rear of the base. If the horizontal force is generated from internal leg forces, the effect of the horizontal force on the base loading distribution will be height dependent, since the leg changes inclination with height. For the 80-in test height, the base resultant with horizontal forces generated by the internal leg force acted at about 65 in from the rear of the base. Therefore, for this shield configuration, horizontal loading moved the resultant approximately 10 in toward the rear of the base. The resultant location starts near the leg and migrates toward the toe as loading increases. The migration toward the toe is suppressed when horizontal loading is present, causing the resultant to act closer to the leg. A comparison of base loading distribution with and without horizontal loading is shown in figure 19.

In summary, if the immediate roof and floor are capable of restraining the natural tendency of the canopy and base to displace horizontally from the action of the leg forces, horizontal loading will be developed that will reduce toe loading. On the other hand, if there is loose debris on the canopy or under the base, the canopy and base may not be restrained and toe loading will be greater. The increase in toe loading caused by the lack of restraining horizontal force varies depending on the magnitude of the horizontal force developed and the shield geometry. For the example shown in figure 19, toe pressure was found to increase by about 75 pct when the horizontal loading was completely eliminated.

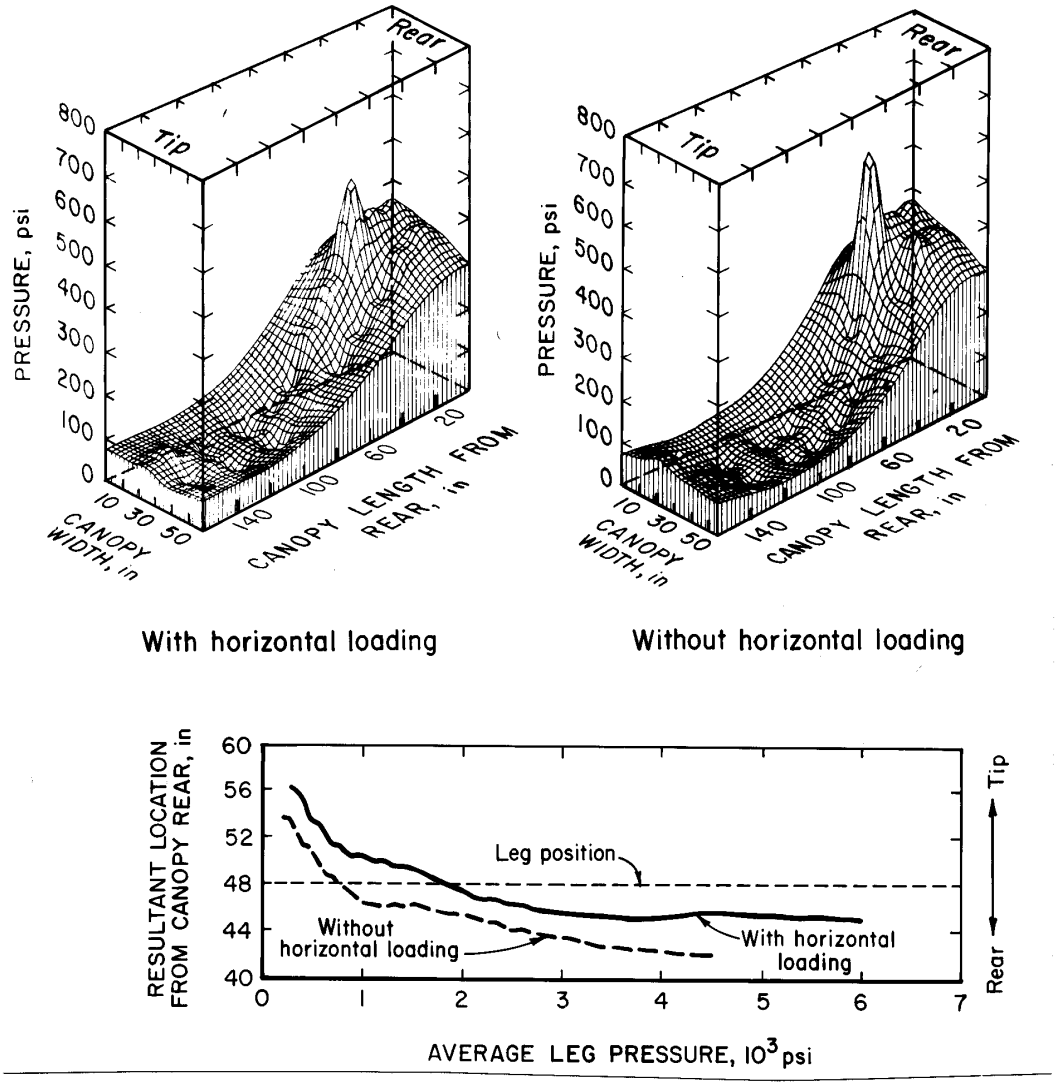

Figure 18.—Comparison of canopy resultant locations with and without horizontal loading.

Tests were conducted to determine the effect of the base-lifting device on the base loading distribution. The base-lifting device is a 1.5-in-thick plate that is placed under the toes of the base. It is hydraulically activated to lift the toes of the base during support advance. Although the device is inactive during the mining cycle, it promotes two-point contact at the toe and rear of the base, which causes greatly increased loading in these areas.

Since the base units are very stiff, the base does not deform sufficiently to provide more uniform contact. Hence, the resulting load distribution is highly dependent upon the compliance of the immediate floor; toe loading increases with increased floor stiffness. The compliance of the floor was simulated by placing 3/4 in of plywood between the load cells and the base. The 3/4 in of wood was insufficient to permit full contact along the length of the base. Hence, the resulting distribution was bimodal with areas of higher stress at the toe and rear of the base. However, the loading at the toe was typically an order of magnitude greater than the loading at the rear of the base. Maximum pressures at the toe of the support were on the order of 7,500 psi when distributed over the 36 in^2 of load cell area.

Figure 20 compares base load development with and without the base-lifting device. For these particular tests, maximum toe loading increased by 215 pct from 35 to 110 tons at 4,000 psi of leg pressure, while the load at the rear of the base increased by an order of magnitude from about 2 tons to 25 tons.

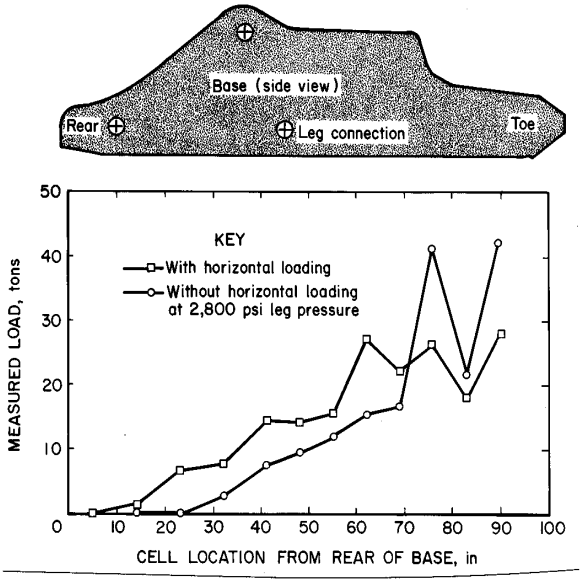

Figure 19.—Comparison of base loading with and without horizontal loading.

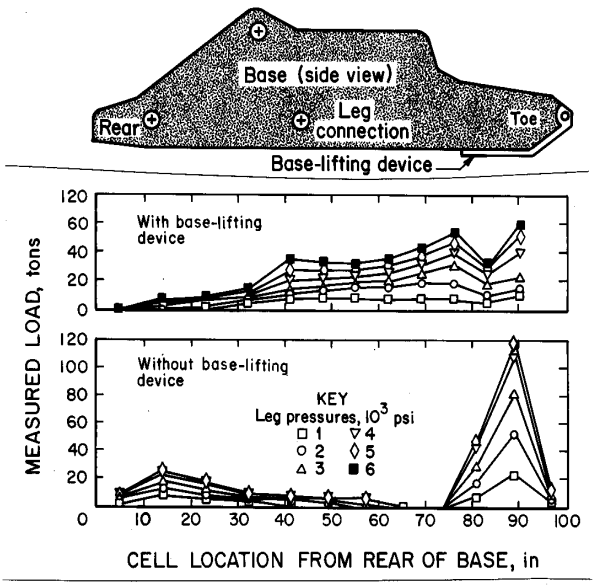

Figure 20.—Comparison of base loading with and without base-lifting device.

To provide more compliancy in the floor, 2.5 in of rubber was used between the base and load cell on one test. However, the rubber columns tended to shear from the action of the leg forces pushing the base horizontally, rather than compressing the rubber vertically as intended. The end result was a reduction in horizontal force acting on the base, which caused increased toe loading and reduced pressure at the rear of the base.

To determine the effect of the canopy contact configuration on the base loading distribution, an effort was made to control the resultant location on the canopy by placing contact blocks at certain locations on the canopy. However, as previously indicated, the resultant location on the canopy must be in close proximity to the leg to maintain equilibrium. Hence, the base pressure was not significantly affected by the changes in the canopy contact as shown in figure 21. Since the location of the resultant force on the canopy is dependent upon the canopy capsule force, the capsule force was varied over its full range. As shown in figure 22, the change in canopy capsule force moved the location of the resultant force acting on the base approximately 12 in. As the capsule force decreases, the canopy resultant moves closer to the leg, causing the base resultant to move closer to the toe.

An example of the base contact pressure for full-contact loading is illustrated in figure 23. The pressure profile is fairly linear between the rear and the toe when the base-lifting device is removed and horizontal shield loading is present. Peak toe pressures are typically in the range of 400 to 500 psi for leg pressures approaching 6,000 psi, while pressures at the rear of the base are typically in the neighborhood of 50 to 100 psi. As previously indicated, the absence of horizontal loading can affect these contact pressures by about 75 pct. The pressure profile is more nonlinear with higher toe loading when the horizontal forces are eliminated. A comparison of contact pressure profiles with and without horizontal loading is shown in figure 24. Toe pressures of 700 to 800 psi were calculated at leg pressures of about 3,000 psi with the base-lifting device installed, and peak pressures at the initial contact locations were in the range of 1,500 to 1,750 psi. It is important to remember that these values are determined by distribution of the measured load cell forces over the complete area of the base. If less than full contact is attained, significantly higher contact pressures can be developed.

Combined Canopy and Base Tests

A series of tests were conducted in which both the canopy and base contact loads were measured. Five combinations of canopy and base contact configurations as shown in figure 25 were evaluated. A primary purpose of this test series was to evaluate the interaction of the canopy and base contact conditions. Another objective was to determine the canopy and base loading for two-point contact on both components, since this is likely to be the configuration that produces maximum loading. The third objective was to simulate a reported common contact configuration at the mine site where the shield was used, that is, full base contact with full canopy contact except for the sloped portion of the canopy tip. A final objective of

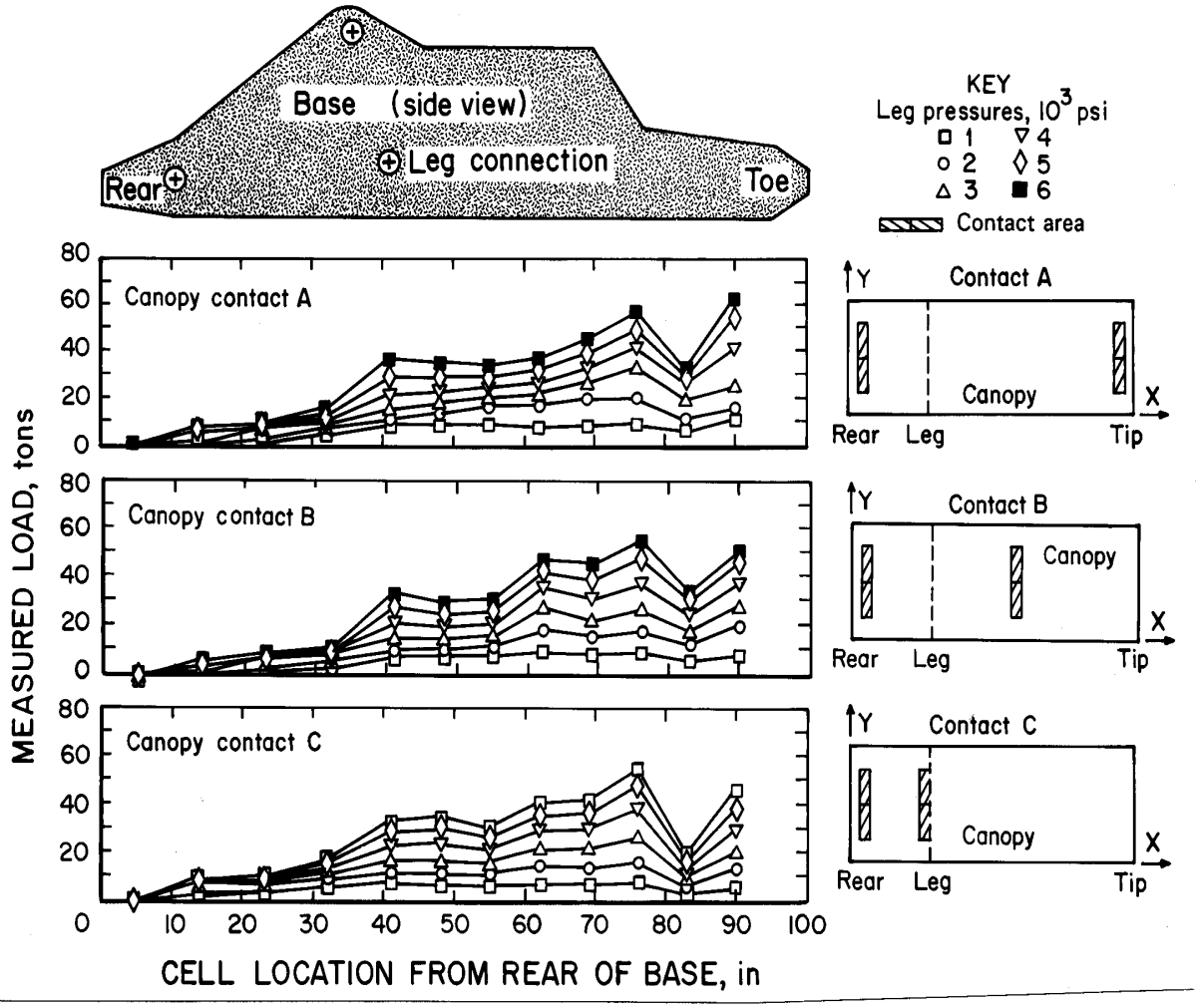

Figure 21.—Effect of canopy resultant location on base loading.

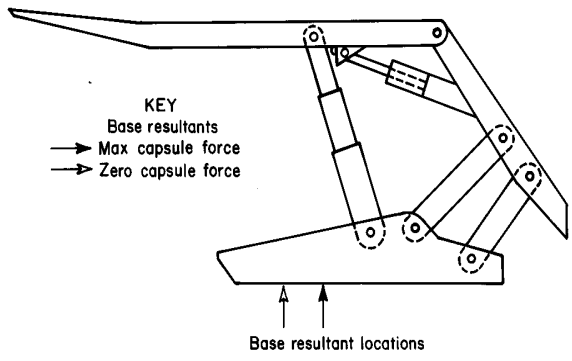

Figure 22.—Effect of canopy capsule force on base resultant.

the combined canopy and base series was to evaluate the effects of face-to-waste strata movements on the canopy and base loading distribution.

Using the scheme that was developed for the base series of tests, an effort was made to vary the resultant location on the canopy by varying the canopy contact configuration. Seven pressure cells evenly spaced under each base unit were used to simulate full base contact for these tests. The resultant locations on the canopy and base for these three tests are shown in figure 26. As seen in the figure, the resultant location on the canopy migrated to a position 2 to 3 in behind the leg at leg pressures above 5,000 psi. With contact at the canopy tip, the canopy resultant was as much as 12 in closer to the rear of the canopy at leg pressures below 1,700 psi than in other

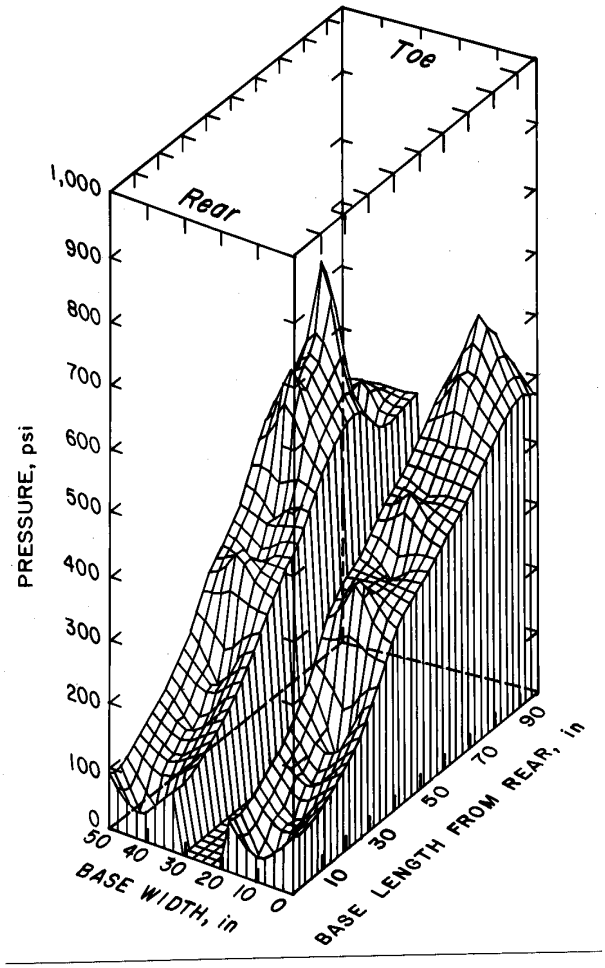

Figure 23.—Contact pressure profile for base.

configurations where there was no contact at the tip of the canopy. This difference in canopy resultant shifted the base resultant slightly toward the rear by about 2 in at low leg pressures.

Load development and contact pressure profiles on the base were similar for these three canopy contact configurations (see figure 27). Slightly higher toe loading on the base was produced at high leg pressures for the canopy configuration with tip contact. Load development and contact pressure profiles for the canopy were significantly different, since the contact configuration was different for all three tests. As shown in figure 28, maximum contact loading was developed for the configuration where a line of contact was established near the leg, since little force was required at the rear of the canopy to maintain equilibrium. The most uniform canopy loading was established when the canopy contacts were equally spaced from the leg connection.

Figure 29 shows load development for two-point canopy and base contact. Maximum loads were developed at the rear of the canopy and toe of the base. Total loading at the rear of the canopy at 5,000 psi leg pressure was 475 tons. Distributed over the 180 in^2 of contact area provided by the load cells, this translates into approximately 5,300 psi. Total load at the tip of the canopy was 117 tons, which equates to 1,300 psi. Total load on the toe of the base units was 235 and 200 tons, which equates to approximately 6,500 and 5,600 psi, respectively, for the 72 in^2 of contact area, while loading at the rear of the base was 83 and 115 tons or 2,300 and 3,200 psi.

The test configuration with canopy contact over the first 80 in, beginning from the rear (approximately 50 pct of the canopy area with no tip contact), produced a stress concentration at the leg connection as shown in figure 30. Maximum loads of 280 tons were developed in the two load cells at this location, producing a contact pressure of about 7,800 psi.

Horizontal shield loading is developed by horizontal displacement of the canopy relative to the base. Since the leg is inclined toward the face, the natural tendency is for the canopy to be pushed toward the face. When this motion is permitted without resistance from the roof, there is no external force acting on the shield. When the forward motion of the canopy is restrained by the roof, this restraining force acts as a horizontal force on the shield. Conversely, if the strata move toward the face and sufficient friction is generated at roof and floor shield interfaces, the canopy will be displaced backward toward the gob, creating a horizontal force acting on the shield.

Hence, three horizontal displacements of the canopy relative to the base are possible: (1) toward the face, (2) no displacement, and (3) toward the gob. Each of these conditions causes a change in the reactions developed at the canopy-caving shield joint and lemniscate link forces, which affect the load distribution on the canopy and base. A comparison of canopy and base resultant force locations for these conditions is shown in figure 31. Movement of the canopy toward the gob (face-to-waste strata displacement) caused the canopy resultant to move slightly forward toward the tip where it acted closer to the leg in comparison to the condition where the canopy was horizontally constrained or where the canopy was permitted to freely displace toward the face. A much greater effect was seen on the base resultant because of the change in link forces. The base resultant acted closest to the toe when the canopy was permitted to displace freely toward the face, and moved progressively away from the toe toward the rear as the canopy was horizontally restrained and then forced to

move toward the gob. The base resultant locations for these three conditions are as follows: (1) for movement of the canopy toward the face, the resultant was located 22 in from the toe; (2) for no horizontal movement of canopy relative to the base, the resultant was 41 in from the toe; and (3) for movement of canopy toward the gob, the resultant was 49 in from the toe.

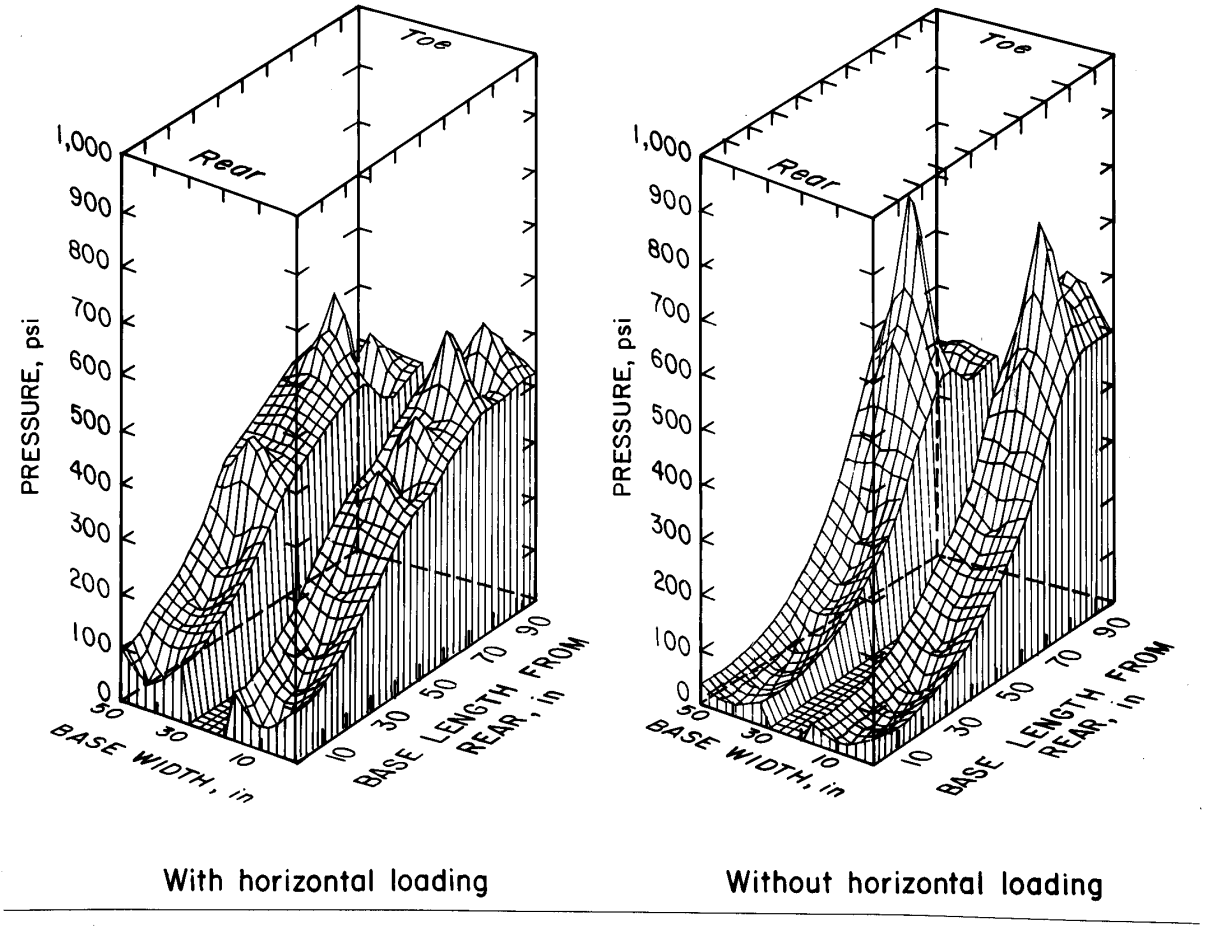

Figure 24.—Comparison of base contact pressure profile with and without horizontal loading.

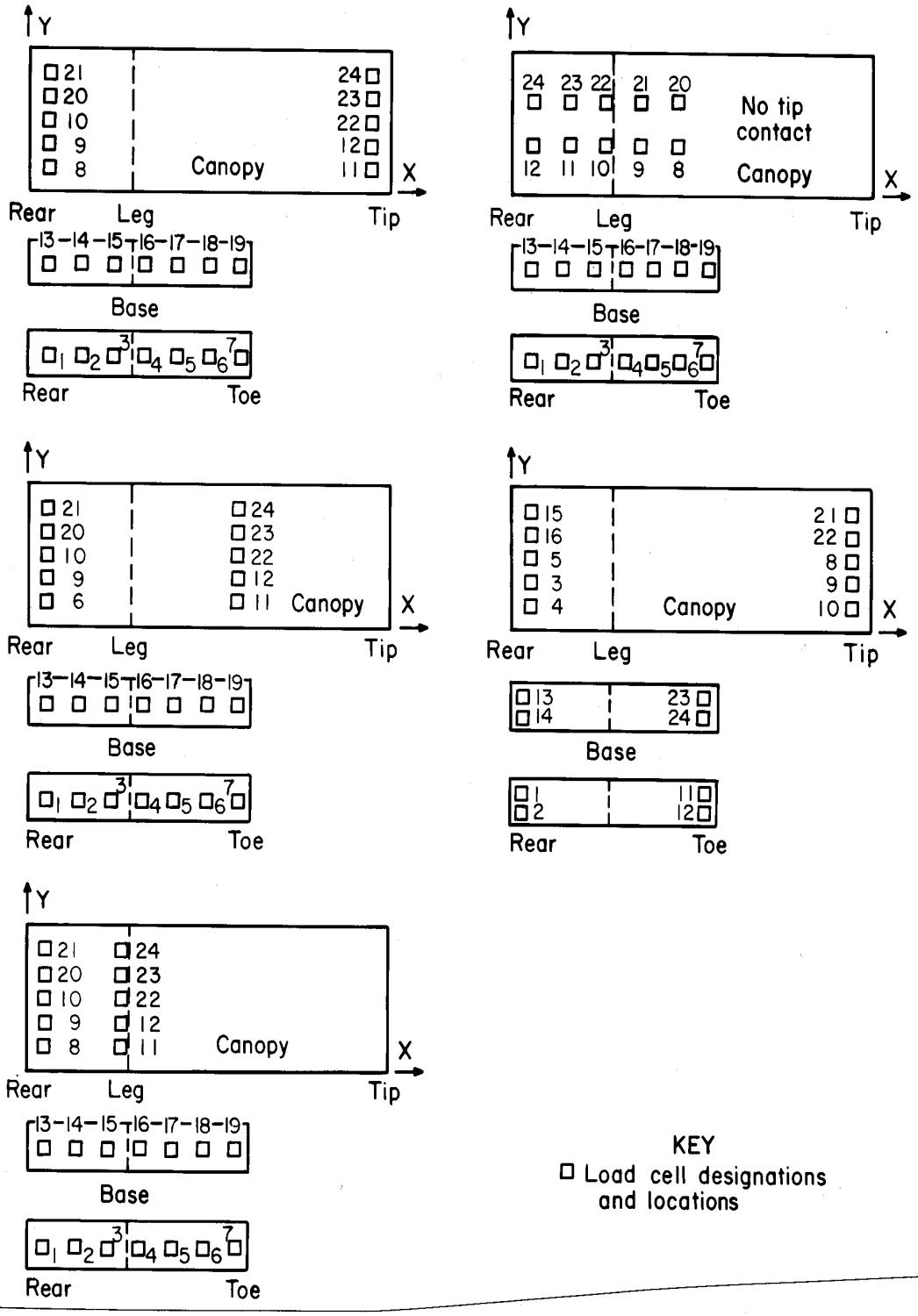

Figure 25.—Combinations of canopy and base contact configurations.

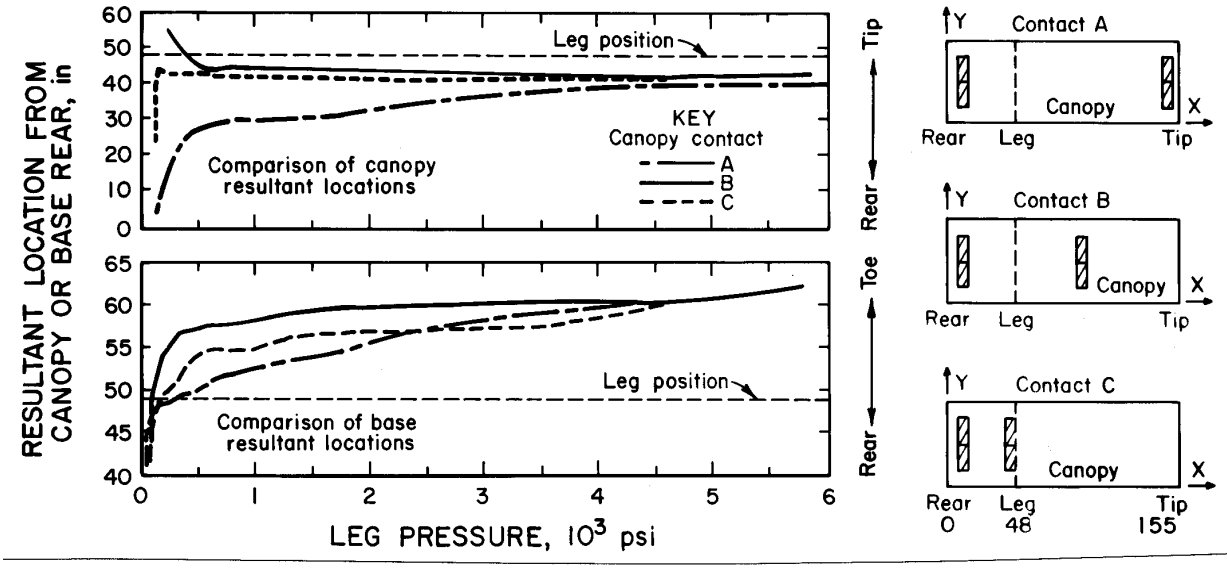

Figure 26.—Comparison of canopy and base resultant force locations.

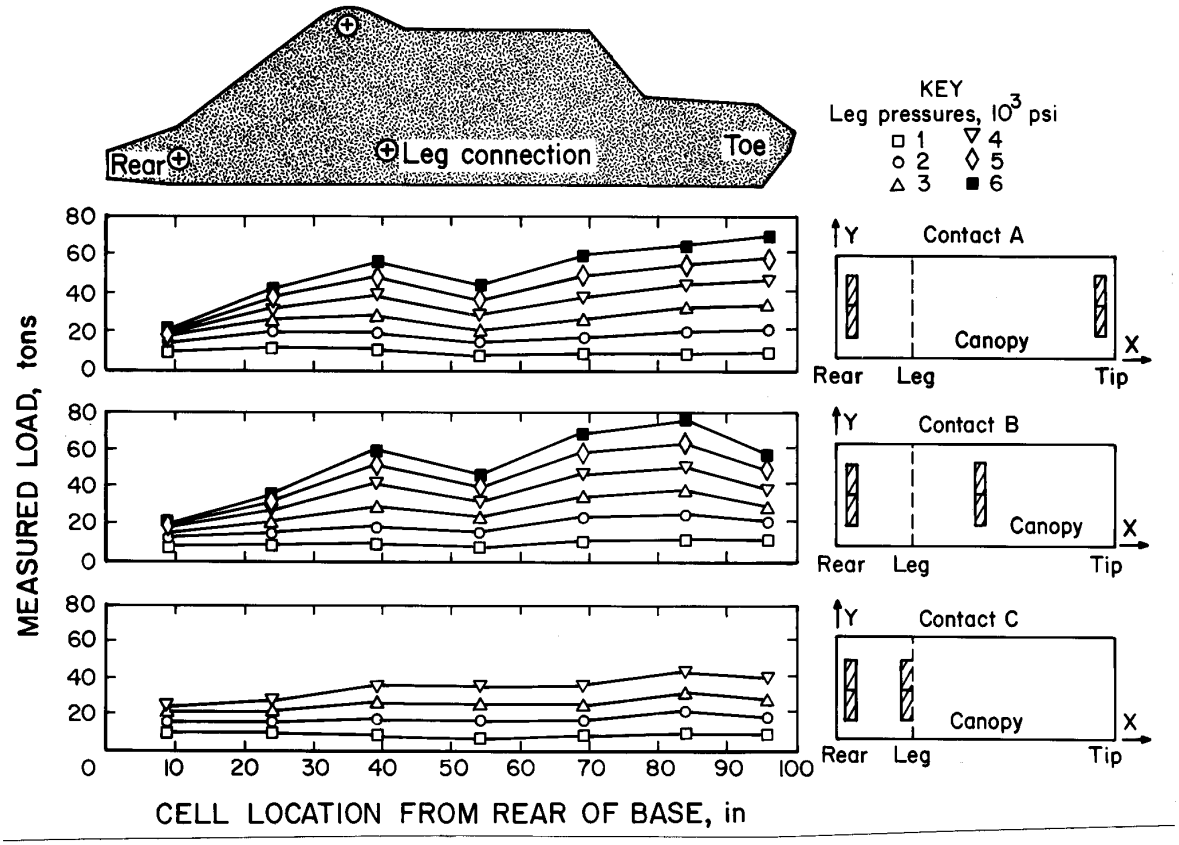

Figure 27.—Load development for controlled canopy resultant tests.

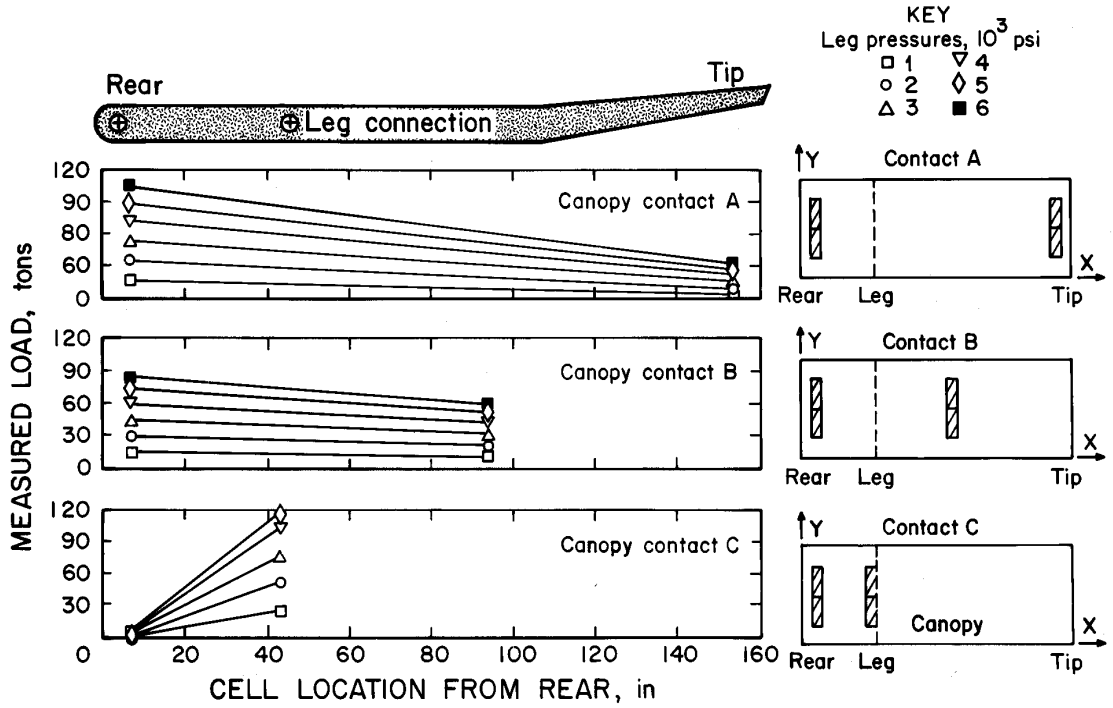

Figure 28.—Maximum contact loading for controlled canopy resultant tests.

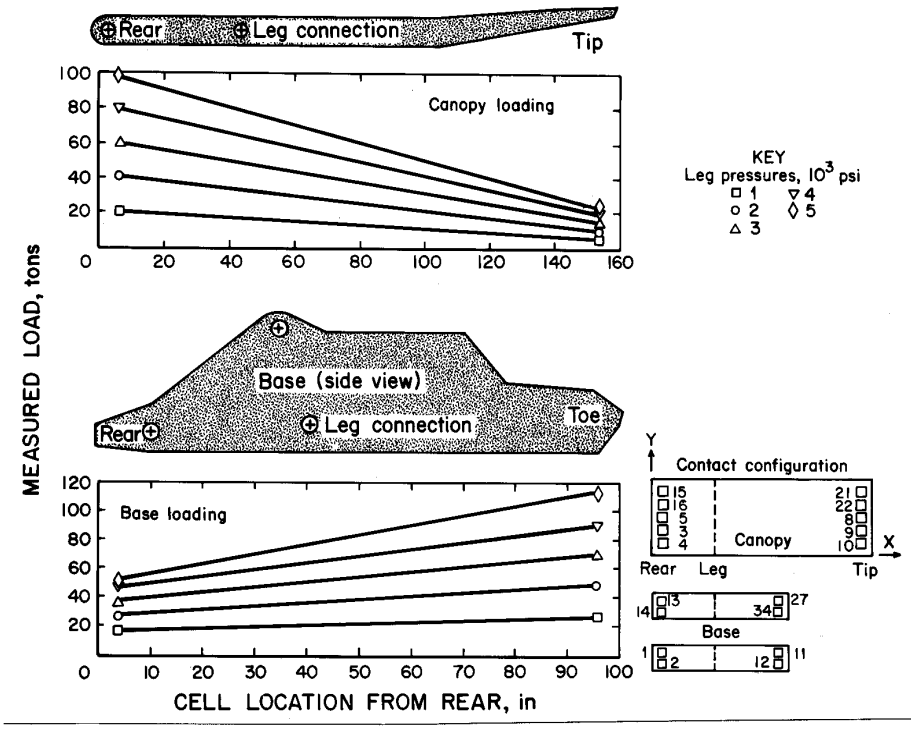

Figure 29.—Load development for two-point canopy and base contact.

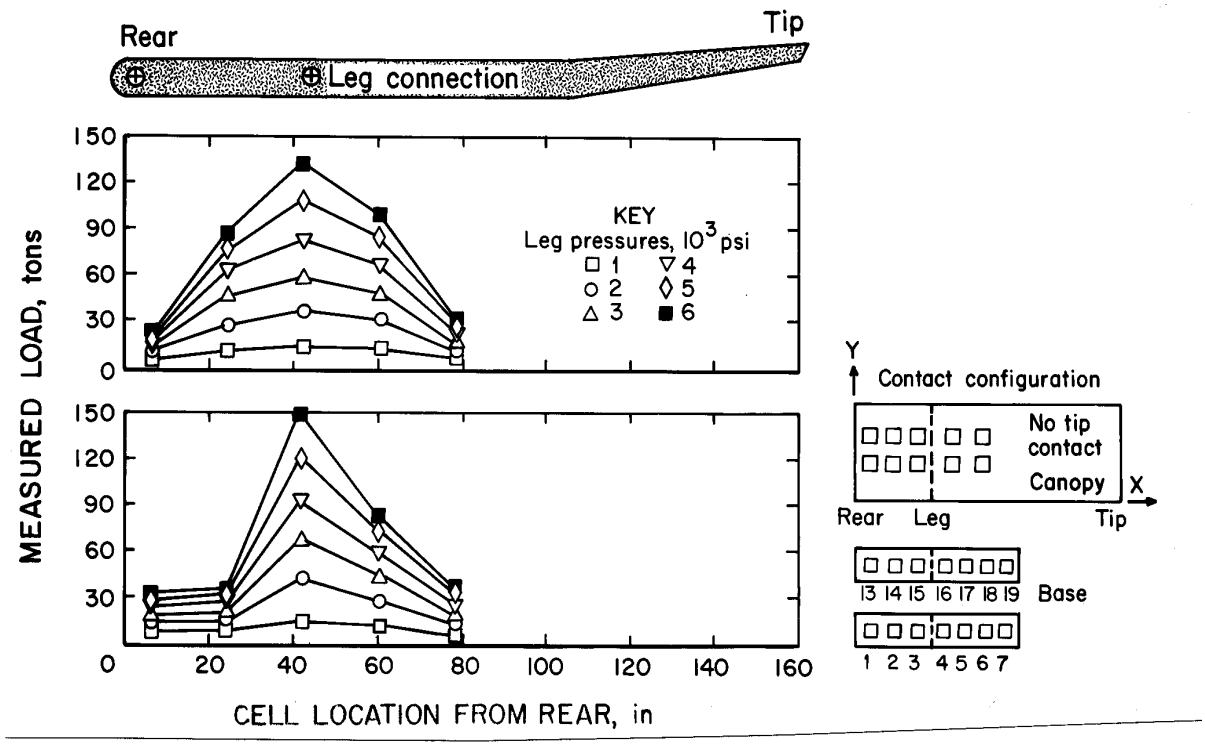

Figure 30.—Load development in absence of canopy tip contact.

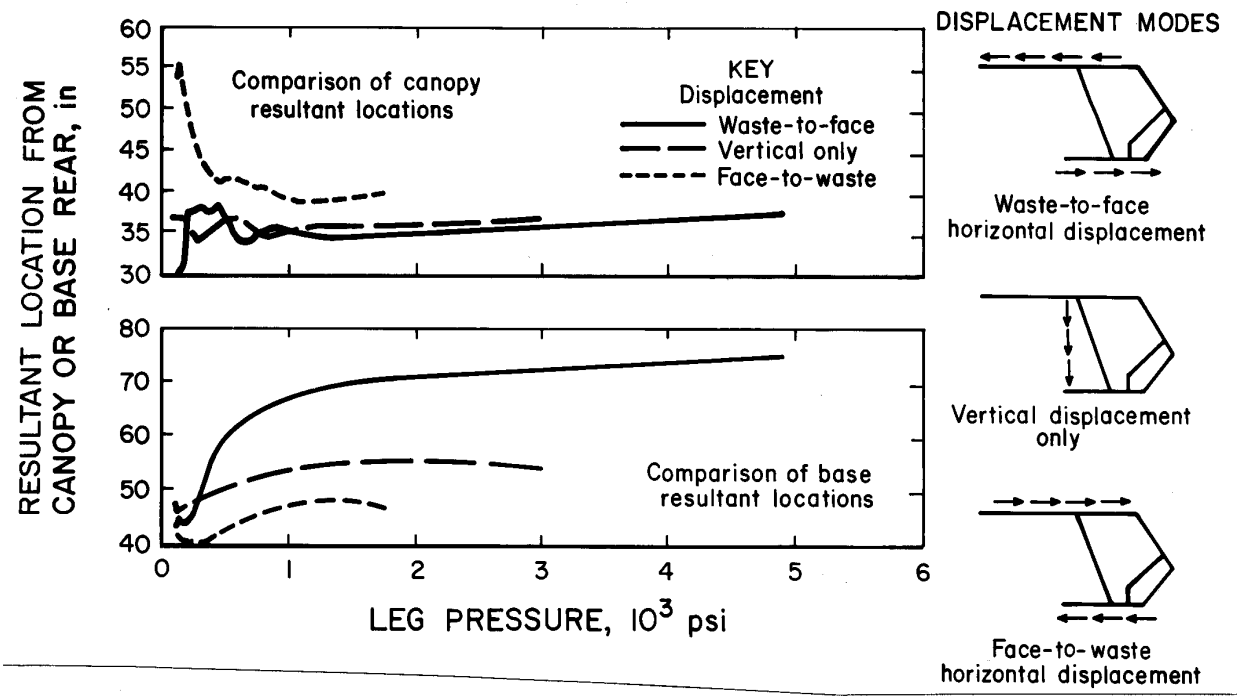

Figure 31.—Effects of horizontal displacements of the canopy on the canopy and base resultant force locations.

SUMMARY AND CONCLUSIONS

The distribution of internal shield forces to the immediate roof and floor can be a critical element in the capability of a shield to provide effective ground control. While shield roof and floor contact pressures are normally rated assuming a uniform load distribution on the canopy and base, underground utilization produces contact pressures of much greater magnitude because the load distribution is not uniform. The contact configuration and the actual load distribution is largely dependent upon the compliancy of the strata, which is difficult to simulate in the laboratory.

Assuming the contact configuration established between the shield and the immediate strata is properly simulated, the profile of the resulting load distribution on the shield can be determined by placing an array of load-measurement devices on the canopy and base. However, an accurate assessment of the magnitude of the contact pressure is more difficult to obtain, since the load-measuring instrumentation typically covers only a small percentage of the total canopy and base contact area and the magnitude is highly dependent upon this contact area. The approach taken in this study was to distribute the load measured from 24 hydraulic pressure cells over the entire area of the canopy and base using a stress contour software program. The difficulty in this approach is that most stress contour programs are designed to interpolate between data points. Therefore, it is necessary to scale measured loads in proportion to the percentage of measured contact area to preserve force equilibrium when extrapolating to full-contact load conditions.

Because the canopy tip is sloped upward and a base-lifting device is employed, the actual contact area that is achieved underground with this particular shield design is largely dependent upon the compliancy of the immediate roof and floor. It is concluded that full contact on the canopy and base is not achieved without deformation of the strata, suggesting that high contact pressures are developed at the ends of the canopy and base for very competent (stiff) immediate roof and floor strata.

The loading distribution changes in both magnitude and profile as the loading on the shield increases. The general tendency is for initial loads to be concentrated at the ends of the canopy and base, and then to migrate to other areas as increased loading causes additional contact. For leg pressures above setting pressures, the general load distribution is a continually increasing pressure from the canopy tip to the canopy rear and decreasing pressure from the toe of the base to the rear of the base. A linear approximation can be used, but a nonlinear approximation is more accurate, particularly when horizontal forces are removed.

Relatively little force is developed at the tip of the canopy compared with the rear of the canopy, largely due to the fact that the tip is located farther from the leg than the rear of the canopy is and partially due to the flexibility of the canopy. This arrangement requires considerably more force at the rear than is required at the tip to maintain moment equilibrium. The canopy capsule controls tip loading, but only at low leg pressures, and is generally ineffective at leg forces above setting pressure. Maximum loads are developed at the rear of the canopy, with a migration of this maximum toward the leg as the immediate strata deform.

The inclination of the tip promotes initial contact of the tip and discourages contact between the tip and leg. If the goal is to develop maximum tip loading, this design is warranted since tip loading is maximized when the contact pressure near the leg is limited. However, structurally this configuration induces large amounts of bending strain that cause high stress concentrations in the canopy for most load conditions. Even with this design, the amount of force generated at the canopy tip is rather small, about 10 pct of the total shield capacity for stiff roof conditions and less than 5 pct for more compliant roof and floor structures. The most efficient method to increase tip loading is to shorten the distance from the tip to the leg, but the capacity to do this is limited by the requirement to minimize the exposed tip-to-face distance and the limitation on extending the length of the base due to the location of the face conveyor.

The canopy is cantilevered in front of the toe of the base and the leg is inclined so that the leg connection on the canopy is forward of the leg connection on the base. This geometry induces a rotational moment that promotes high load concentrations at the toe of the base. A face-to-waste external horizontal load acting on the canopy reduces the concentration of toe loading. This horizontal loading can be produced by face-to-waste movement of the immediate roof or by frictional force developed at the roof interface, which resists the natural tendency of the canopy to be pushed toward the face by the leg forces. Hence, friable strata that develop a layer of debris on the canopy is more likely to produce high toe loading than more competent strata that resist the shearing forces developed at roof interface.

The base-lifting device exaggerates the inherently high toe loading on the base. The design of the base-lifting device could be improved to eliminate the debris that builds up between the lifting plate and the base structure. This debris prevents the full retraction of the base-lifting device, which further aggravates the toe loading problem. A more

effective design from the perspective of the loading distribution on the base would be to have the device located where it would not be in contact with the base-bearing surface. One possibility would be to place a similar device between the two base pontoons.

Unlike the canopy, where the resultant vertical force is fixed in location at close proximity to the leg, the resultant location on the base theoretically could be controlled if the link forces could be controlled. This suggests that toe loading might be reduced if the link forces could be reduced to cause the resultant force to act closer to the leg. Additional research would help to evaluate this concept in more detail.

APPENDIX.—DISTRIBUTION OF MEASURED CONTACT FORCES

The software package used to process the data from the pressure cells uses the inverse distance squared function to distribute the measured forces over the unmeasured areas of the canopy and base to estimate the actual contact pressure distribution if measurements were available over the entire canopy or base surface. In order to simulate full contact load conditions and to preserve force equilibrium, the measured forces from the load cells must be reduced in magnitude in proportion to the area covered by the load cells relative to the total canopy or base surface area. Otherwise, the stress contour program would preserve the measured forces at the load cell and by interpolating between load cells produce a total loading that exceeds the actual total load applied to the shield. The profile of loading is then determined by superpositioning of all distributed forces from the load cells as determined by the inverse distance squared relationship.

Since the program preserves the measurement at the location where it is recorded, a smooth distribution is generally not achieved. The peaks and valleys that appear in the stress distribution plots are an artifact of the distribution process. Low values in close proximity to large values appear as dimples below the surface, while the larger value is distributed around the lower value. Likewise, large values appear as peaks. Hence, the actual contact pressure is likely to be between the smooth surface of the distribution shown in the contour plots and the peaks and valleys.

The equation for the inverse distance squared function is

$$Z = \frac{\sum_{i=1}^{n} \frac{Z_i}{d_i^2}}{\sum_{i=1}^{n} \frac{1}{d_i^2}},$$

where Z = neighboring measured point,

d = distance,

and n = number of Z elements.